

charging event will always be dressed by the reorganization of the system in nearby sites (26).

References and Notes

1. E. Abrahams, P. W. Anderson, D. C. Licciardello, T. V. Ramakrishnan, *Phys. Rev. Lett.* **42**, 673 (1979).
2. S. V. Kravchenko, G. V. Kravchenko, J. E. Furneaux, V. M. Pudalov, M. D'lorio, *Phys. Rev. B Cond. Matter* **50**, 8039 (1994).
3. For a comprehensive review of the MIT in 2D, see E. Abrahams, S. V. Kravchenko, M. P. Sarachik, *Rev. Mod. Phys.* **73**, 251 (2001).
4. S. Ilani, A. Yacoby, D. Mahalu, H. Shtrikman, *Phys. Rev. Lett.* **84**, 3133 (2000).
5. Y. Hanein et al., *Phys. Rev. Lett.* **80**, 1288 (1998).
6. M. J. Yoo et al., *Science* **276**, 579 (1997).
7. Y. Y. Wei, J. Weis, K. V. Klitzing, K. Eberl, *Phys. Rev. Lett.* **81**, 1674 (1998).
8. N. B. Zhitenev et al., *Nature* **404**, 473 (2000).
9. J. P. Eisenstein, L. N. Pfeiffer, K. W. West, *Phys. Rev. Lett.* **68**, 674 (1992).
10. S. Shapira et al., *Phys. Rev. Lett.* **77**, 3181 (1996).

11. The critical density was determined by simultaneous measurement on the same device, with the same technique as in (4).
12. S. C. Dultz, H. W. Jiang, *Phys. Rev. Lett.* **84**, 4689 (2000).
13. A possible explanation of this behavior, which relates it to effects of disorder, has been given by Si and Varma [Q. Si, C. M. Varma, *Phys. Rev. Lett.* **81**, 4951 (1998)].
14. B. L. Altshuler, D. L. Maslov, V. P. Pudalov, preprint available at xxx.lanl.gov/abs/cond-mat0003032.
15. A. L. Efros, B. I. Shklovskii, *J. Phys. C Solid State Phys.* **8**, L49 (1975).
16. S. He, X. C. Xie, *Phys. Rev. Lett.* **80**, 3324 (1998).
17. Y. Meir, *Phys. Rev. Lett.* **83**, 3506 (1999).
18. An electron crystal, which is suggested by several theories (19–23) to appear at the MIT, might produce both continuous and discrete behaviors. Generally, the crystal deforms continuously to screen an external potential, producing a continuous response. However, occasionally, electrons collectively reorganize around pinning centers (24), causing an abrupt reduction of energy and hence a spike in  $\delta\mu/\delta V_{BG}$ . In this scenario, a single spike corresponds to a many-electron

tron charging event, rather than a single-electron charging, as in previous scenarios.

19. B. Tanatar, D. M. Ceperley, *Phys. Rev. B* **39**, 5005 (1989).
20. S. T. Chui, B. Tanatar, *Phys. Rev. Lett.* **74**, 458 (1995).
21. G. Benenti, W. Xavier, J. L. Pichard, *Phys. Rev. Lett.* **83**, 1826 (1999).
22. S. Chakravarty, S. Kivelson, C. Nayak, K. Voelker, *Philos. Mag. B* **79**, 859 (1999).
23. J. Yoon, C. C. Li, D. Shahar, D. C. Tsui, M. Shayegan, *Phys. Rev. Lett.* **82**, 1744 (1999).
24. I. M. Ruzin, S. Marianer, B. I. Shklovskii, *Phys. Rev. B Cond. Matter* **46**, 3999 (1992).
25. The value of  $s_{min}$  could be estimated from the ratio of capacitances between the 2DHG and the top and back gates to be  $s_{min} = 2.3$ .
26. M. Pollak, M. Ortuno, in *Electron-Electron Interactions In Disordered Systems*, A. L. Efros, M. Pollak, Eds. (North-Holland, Amsterdam, 1985), vol. 10, pp. 287–408.
27. We benefited from discussions with M. Brodsky, A. M. Finkel'stein, Y. Imry, Y. Meir, A. Stern, C. M. Varma, and N. B. Zhitenev. This work was supported by the MINERVA Foundation, Germany.

27 December 2000; accepted 4 April 2001

# Controlling Chemical Turbulence by Global Delayed Feedback: Pattern Formation in Catalytic CO Oxidation on Pt(110)

Minseok Kim, Matthias Bertram, Michael Pollmann, Alexander von Oertzen, Alexander S. Mikhailov, Harm Hinrich Rotermund,\* Gerhard Ertl

Control of spatiotemporal chaos is one of the central problems of nonlinear dynamics. We report on suppression of chemical turbulence by global delayed feedback using, as an example, catalytic carbon monoxide oxidation on a platinum (110) single-crystal surface and carbon monoxide partial pressure as the controlled feedback variable. When feedback intensity was increased, spiral-wave turbulence was transformed into new intermittent chaotic regimes with cascades of reproducing and annihilating local structures on the background of uniform oscillations. The global feedback further led to the development of cluster patterns and standing waves and to the stabilization of uniform oscillations. These findings are reproduced by theoretical simulations.

Control theory was originally developed for military and industrial applications, with the task of stabilizing missile trajectories or the course of technological processes (1, 2). Similar approaches are used today to steer elementary physical and chemical systems with chaotic dynamics. To control a chaotic system, its behavior is monitored and subsequent corrective perturbations needed to stabilize a chosen unstable orbit are computed. However, such exact methods (3) require substantial real-time computations and become impractical for the control of fast processes and large systems. An

alternative is provided by empirical methods involving delayed feedback [see, e.g., (4)]. To realize such a feedback, a monitored variable is taken with a fixed time delay and used to generate a control signal that acts back on the system by changing one of its parameters. A feedback is global if the control signal represents a sum of contributions coming from many parts of the system. Various forms of delayed feedback have been discussed in optics, to suppress spatiotemporal instabilities in lasers (5–7). Further examples of global feedback control include suppression of plasma instabilities in gas discharges (8) and effects of charge transport in semiconductors (9). Stabilization of unstable stationary states by delayed feedback in a stirred chemical reactor has also been experimentally demonstrated (10).

In addition to its control function, global

feedback can also be used to modify spatiotemporal pattern formation and produce new kinds of patterns. In reactions of heterogeneous catalysis, some global feedback through the gas phase is intrinsically present and influences pattern formation (11–14). In experiments with artificial global nondelayed feedback in the photosensitive oscillatory Belousov-Zhabotinsky (BZ) reaction (15), formation of spatial clusters has been observed [similar patterns in this reaction are also found under external periodic forcing (16)].

Here we focus on experimental and theoretical investigations of the effect of global delayed feedback on chemical turbulence. In oscillatory reaction-diffusion systems, this form of turbulence results from the difference in diffusion constants of reactants. If this difference is sufficiently large, uniform kinetic oscillations may become unstable and spatiotemporal chaos sets in (17). In the developed turbulent state, both the amplitude and the phase of local concentration oscillations are strongly fluctuating. A characteristic property of such turbulence is spontaneous creation of multiple rotating spiral waves. This diffusion-induced turbulence is typical for oscillatory surface chemical reactions (18, 19) and has also been observed under special conditions in the BZ reaction (20). On the basis of theoretical investigations of a general mathematical model, it was previously suggested (21, 22) that this form of turbulence can be suppressed by application of an appropriate global delayed feedback and that the feedback can also produce new kinds of spatiotemporal patterns. Here, we demonstrate the operation of global delayed feedback in an experiment with catalytic oxidation of CO on platinum.

In contrast to other oscillatory chemical reactions, the mechanism of CO oxidation on Pt(110) is relatively simple (19). Molecules of CO and O<sub>2</sub> adsorb from the gas phase on the catalytic metal surface (the adsorption of O<sub>2</sub> is

Abteilung Physikalische Chemie, Fritz-Haber-Institut der Max-Planck-Gesellschaft, Faradayweg 4-6, 14195 Berlin, Germany.

\*To whom correspondence should be addressed. E-mail: rotermund@fhi-berlin.mpg.de

dissociative). Adsorbed CO molecules diffuse and react with O to produce CO<sub>2</sub>, and subsequently CO<sub>2</sub> desorbs from the surface. An interplay of reaction, lateral diffusion of reactants, and adsorbate-induced surface reconstruction (affecting adsorption kinetics of oxygen) gives rise to various two-dimensional (2D) concentration patterns that can be directly imaged with electron or optical microscopy methods (23, 24). The observed reaction-diffusion patterns are highly sensitive to the partial pressures of CO and O<sub>2</sub> in the gas phase ( $p_{\text{CO}}$  and  $p_{\text{O}_2}$ ).

In our experiments, the Pt(110) single-crystal sample was kept in an ultrahigh-vacuum (UHV) apparatus (25). Gas supplies for CO and O<sub>2</sub>, as well as pressure gauges, allowed for controlled dosing of reactants into the UHV chamber. A photoemission electron microscope (PEEM) was used to continuously image lateral distributions of adsorbed species on part of the surface through their respective work-function differences (26). The PEEM monitored pattern formation inside the observation window. Hence, we could introduce a feedback by making the instantaneous dosing rate of CO dependent on real-time properties of the imaged concentration patterns.

The electronic signal controlling the dosing rate of CO was generated by integrating the PEEM intensity over the whole image after a delay by a constant time  $\tau_d$ . The variation of the partial pressure of CO in the chamber followed the temporal modulation of the dosing rate with an additional delay determined by the residence time of gases in the pumped chamber. Thus, a controlled global feedback was introduced, such that  $p_{\text{CO}}(t) = p_0 + \mu[I(t - \tau) - I_0]$ , where  $t$  is time,  $\tau$  is the effective delay time,  $I$  is the integral PEEM image intensity inside the observation window,  $p_0$  and  $I_0$  are the partial CO pressure and the average base level of the integral PEEM image intensity in the absence of feedback, and the coefficient  $\mu$  determines the feedback intensity (27).

In the experiments, the reaction parameters were chosen in such a way that, in the absence of feedback, the CO oxidation reaction was in the oscillatory regime. Uniform oscillations were, however, unstable, and spontaneous formation of spiral waves was observed. Such spiral waves were repeatedly undergoing breakups, leading to a complex pattern of chemical turbulence. Starting from this regime, global feedback of a fixed intensity was applied in our experiments. Figure 1A shows its effect on the spiral-wave turbulence. The three frames (top row) present PEEM images taken at three subsequent times. The space-time diagram (middle row) displays the temporal evolution of the pattern in the cross section along the line  $ab$ , indicated in the first frame. Below, the horizontal bar displays  $p_{\text{CO}}(t)$  in the reaction chamber (black line) and the total PEEM intensity (red line) during the experiment. Initially,  $p_{\text{CO}}$  is almost constant, but then pressure oscillations

start to grow and reach an amplitude of about 10%. As the global feedback becomes more efficient, spiral-wave turbulence is gradually suppressed, and eventually uniform reaction oscillations set in.

Depending on the reaction and feedback parameters, the feedback does not transform spiral-wave turbulence to stable uniform oscillations, but leads to the formation of new spatiotemporal patterns (Fig. 1, B to D). One of the typical observed regimes, which can be characterized as intermittent chemical turbulence (Fig. 1B), started as a dark, uniform state that then developed small, brighter spots at random locations. When the spots reached a certain size, darker regions developed in the middle of such structures and they transformed into a set of expanding “bubbles.” After some time, the whole pattern faded away and was replaced by the uniform dark state, after which the entire cycle was repeated. To illustrate the temporal

evolution of the pattern, we also show the space-time diagram along the line  $ab$ . Expanding bubbles are represented by triangular structures in this cross section. Examining the diagram, we note that the bubbles could die and reproduce. The bubbles reproduce until many of them are found. Then, massive annihilation occurs and only a few bubbles survive. Thus, an irregular behavior of repeated reproduction is observed. The variation of  $p_{\text{CO}}$  was rigidly correlated with the evolution cycles of the pattern, and  $p_{\text{CO}}$  followed, at a fixed delay, the variation of the integral PEEM intensity.

Phase clusters are shown in Fig. 1C. In this regime, the surface divided into several large domains in which oscillations were shifted by half a period. The pattern was stable and corresponded to periodic oscillations of  $p_{\text{CO}}$ . This regime is similar to the phase clusters previously observed in experiments with the light-sensitive BZ reaction under periodic forcing (16) and

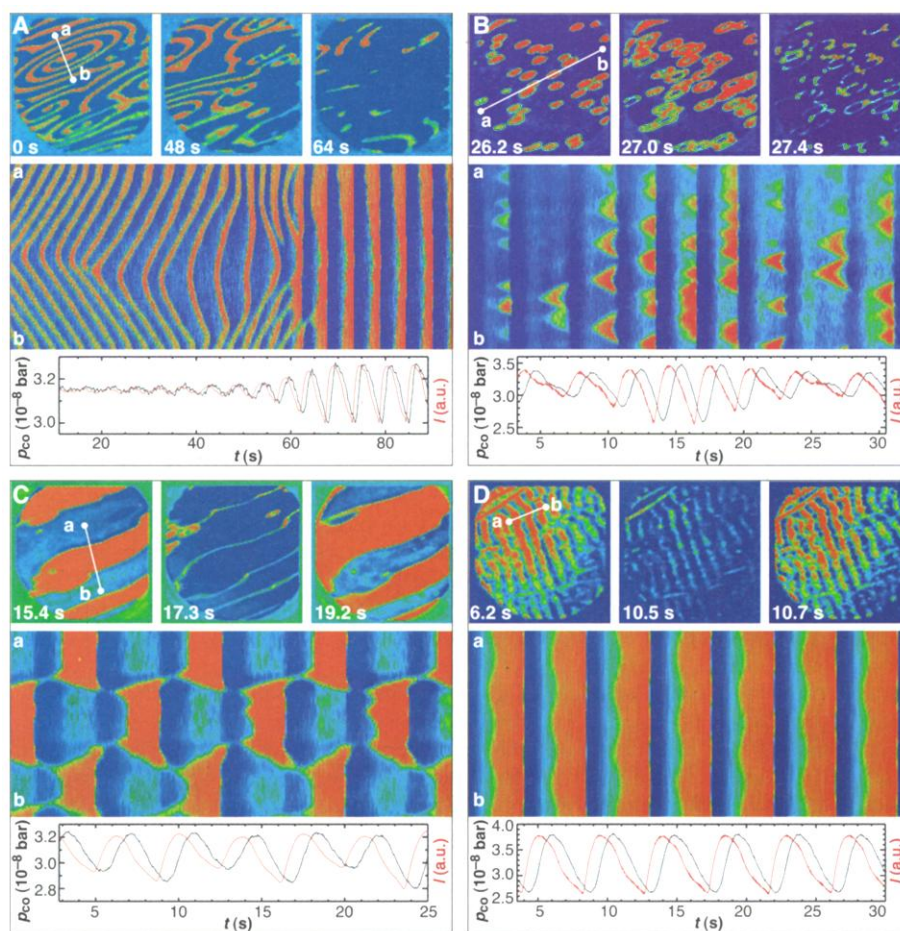


**Fig. 1.** Spatiotemporal patterns observed in experiments with global delayed feedback. **(A)** Suppression of spiral-wave turbulence; **(B)** intermittent turbulence; **(C)** phase clusters; and **(D)** standing waves. In each part, the upper row displays three subsequent PEEM images with a field-of-view of 500  $\mu\text{m}$  in diameter, and images in the middle row are space-time diagrams showing the evolution along the line  $ab$  indicated in the first image. Dark (blue) areas are O covered; brighter (red) regions are mainly CO covered. The horizontal bars under each space-time diagram (bottom row) display the temporal variation of the CO partial pressure (black line) and the variation of the integral PEEM intensity (red line) during the pattern evolution; the time scale is the same as in the diagram. The parameter values of temperature (K), oxygen partial pressure ( $10^{-8}$  bar), base CO pressure  $p_0$  ( $10^{-8}$  bar), feedback intensity  $\mu$  ( $10^{-8}$  bar), and delay time  $\tau$  (s) are, respectively: (A) 498, 10.0, 3.15, 0.8, 0.8; (B) 495, 10.0, 3.15, 2.0, 0.8; (C) 500, 10.0, 3.07, 0.6, 0.8; and (D) 505, 10.0, 3.30, 1.6, 0.8.

global feedback (15). The difference is that local oscillations are period-doubled and the shape of the clusters undergoes weak periodic variation.

Standing waves are displayed in Fig. 1D. In this pattern, bright stripes repeatedly developed from the dark uniform state. The space-time diagram in Fig. 1D shows that the locations of stripes at the next cycle are shifted, and a new stripe develops in the middle between the two stripes seen in the previous cycle. The evolution cycles of the pattern are rigidly correlated with

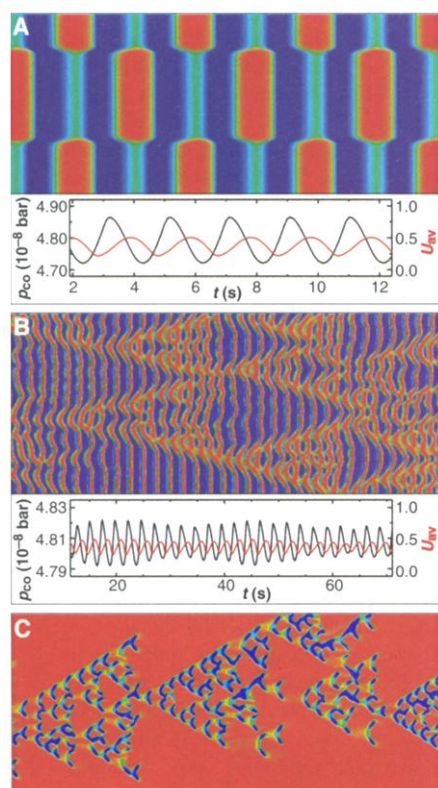


**Fig. 2.** Spatiotemporal patterns in theoretical 1D models with global feedback. **(A)** Phase clusters in the CO oxidation model; the local CO coverage  $u$  is displayed; the system size is  $800 \mu\text{m}$ ; the horizontal bar shows the respective temporal variation of the CO partial pressure (black line) and of the spatial average  $u_{\text{av}}$  (red line). **(B)** Intermittent chemical turbulence in the CO oxidation model; the variable combination  $0.6u - v$  is displayed; half of the pattern in the system of total size  $800 \mu\text{m}$  is shown. **(C)** Intermittent turbulence in the complex Ginzburg-Landau equation with global feedback,  $\partial\eta/\partial t = \eta - (1 + i\beta)|\eta|^2\eta + (1 + i\epsilon)\nabla^2\eta - \mu e^{i\chi(\eta)}$ , where  $\langle\eta\rangle = (1/S)\int\eta dx$  is the spatial average of the complex oscillation amplitude  $\eta$ . The local modulus  $|\eta|$  is displayed; in dimensionless units, the system size is 128 and the shown time interval is 200. The parameters for the patterns (A and B) are  $k_1 = 3.14 \times 10^5 \text{ s}^{-1} \text{ mbar}^{-1}$ ,  $k_2 = 10.21 \text{ s}^{-1}$ ,  $k_3 = 283.8 \text{ s}^{-1}$ ,  $k_4 = 5.86 \times 10^5 \text{ s}^{-1} \text{ mbar}^{-1}$ ,  $k_5 = 1.61 \text{ s}^{-1}$ ,  $s_{\text{CO}} = 1.0$ ,  $s_{\text{O},1x1} = 0.6$ ,  $s_{\text{O},1x2} = 0.4$ ,  $u_0 = 0.35$ ,  $\delta = 0.05$ ,  $D = 40 \mu\text{m}^2 \text{ s}^{-1}$ ,  $\rho_{\text{O}_2} = 13.0 \times 10^{-5} \text{ mbar}$ ,  $p_0 = 4.81 \times 10^{-5} \text{ mbar}$ ,  $u_{\text{ref}} = 0.3358$ , and (A)  $\mu = 0.5 \times 10^{-5} \text{ mbar}$ ,  $\tau = 0.4 \text{ s}$ , (B)  $\mu = 0.12 \times 10^{-5} \text{ mbar}$ ,  $\tau = 0.4 \text{ s}$ . The parameters for the pattern (C) are  $\beta = -1.8$ ,  $\epsilon = 0.8$ ,  $\mu = 0.48$ ,  $\chi = 1.0$ .

the periodic variation of  $p_{\text{CO}}$  in the chamber. Standing waves with such properties can also be observed in this reaction in the absence of artificial global feedback when intrinsic global gas coupling is active (14, 18).

A series of experiments was further performed where the feedback intensity was kept constant and only the delay time was varied (28). The effect of the feedback was sensitive to the delay and, by changing only this parameter, both synchronization and desynchronization of oscillations could be achieved. Moreover, new kinds of patterns, such as localized spiral waves and oscillating cellular structures, were observed with variation of the delay time.

Pattern formation in the CO oxidation reaction on Pt(110) is well described by mathematical models (14, 29, 30). We have found that even a simplified theoretical model predicts the principal effects of the global feedback. The model consists of three equations for the variables  $u$ ,  $v$ , and  $w$  that represent, respectively, the CO and oxygen surface coverages and the local fraction of the surface area found in the nonreconstructed structure:

$$\begin{aligned} \dot{u} &= k_1 s_{\text{CO}} p_{\text{CO}} (1 - u^3) - k_2 u - k_3 uv \\ &+ D \nabla^2 u \\ \dot{v} &= k_4 p_{\text{O}_2} [s_{\text{O},1x1} w + s_{\text{O},1x2} (1 - w)] \\ &(1 - u - v)^2 - k_3 uv \\ \dot{w} &= k_5 [1 + \exp((u_0 - u)/\delta)]^{-1} - k_5 w \end{aligned}$$

The global feedback is introduced assuming that  $p_{\text{CO}}$  is determined as  $p_{\text{CO}}(t) = p_0 - \mu[u_{\text{av}}(t - \tau) - u_{\text{ref}}]$  by the spatially averaged CO coverage  $u_{\text{av}}(t)$  at a delayed time  $t - \tau$ . [The description is a rough simplification because the PEEM intensity actually used in the experiment to compute the control signal is a nonlinear function of both the CO and oxygen coverages, and its form is not exactly known; see (24).] We do not include in the model the weak intrinsic global coupling through the gas phase, because at the relatively high feedback intensities considered here, its effects are negligible. The parameters of the model were chosen in such a way that, in the absence of the feedback, uniform oscillations were unstable and chemical turbulence was observed.

By varying the feedback intensity and the delay time, we found that turbulence could be suppressed and new patterns could be induced by the feedback. Two examples of simulated 1D patterns are shown in Fig. 2, A and B. The properties of the computed cluster patterns (Fig. 2A) are in good agreement with those observed in the experiments, and period doubling of local oscillations is well reproduced. To model standing waves such as those observed, the formation of subsurface oxygen should additionally be taken into account [compare with (14)]. Figure 2B shows an example of a simulation of intermittent turbulence. The cascades of reproducing

and annihilating local structures are clearly seen.

To interpret this result, we show in Fig. 2C a simulation of intermittent turbulence in the complex Ginzburg-Landau equation (CGLE) with global phase-shifted feedback that was previously proposed and investigated by us (21). The CGLE is a general model that describes the behavior of reaction-diffusion systems near onset of self-oscillations, while they remain approximately harmonical. Figure 2C displays the local modulus of the oscillation amplitude in the developing 1D pattern. The turbulent cascades are formed by pairs of amplitude defects (i.e., small regions with greatly decreased oscillation amplitude) that reproduce, annihilate, and travel on the background of almost uniform oscillations. For the respective 2D CGLE with global feedback, the emerging pairs of amplitude defects correspond to growing “bubble” structures (22). Such a pattern of intermittent turbulence agrees with theoretical descriptions (31). Related theoretical models of spatiotemporal intermittency have been analyzed (32).

Thus, our experimental and theoretical investigations indicate that global delayed feedback (through the gas phase) can be used efficiently to control microscopic pattern formation in a surface chemical reaction. In this study, we have focused on chemical turbulence and have demonstrated that it can be completely or partially suppressed by the feedback, giving rise to stable uniform oscillations, intermittent regimes with reproduction cascades of amplitude defects, or regular patterns of clusters and standing waves. Similar effects are expected for other reaction-diffusion systems of different origins.

#### References and Notes

- M. C. Singh, Ed., *Systems and Control Encyclopedia* (Pergamon, New York 1988).
- E. D. Sontag, *Mathematical Control Theory: Deterministic Finite-Dimensional Systems* (Springer, Berlin, ed. 2, 1998).
- E. Ott, C. Grebogi, J. A. Yorke, *Phys. Rev. Lett.* **64**, 1196 (1990).
- K. Pyragas, *Phys. Lett. A* **170**, 421 (1992).
- M. E. Bleich, D. Hochheiser, J. V. Moloney, J. E. Socolar, *Phys. Rev. E* **55**, 2119 (1997).
- M. Munkel, F. Kaiser, O. Hess, *Phys. Rev. E* **56**, 3868 (1997).
- J. Martin-Regalado, G. H. M. van Tartwijk, S. Balle, M. San Miguel, *Phys. Rev. A* **54**, 5386 (1996).
- Th. Pierre, G. Bonhomme, A. Atipo, *Phys. Rev. Lett.* **76**, 2290 (1996).
- G. Franceschini, S. Bose, E. Schöll, *Phys. Rev. E* **60**, 5426 (1999).
- E. C. Zimmermann, M. Schell, J. Ross, *J. Chem. Phys.* **81**, 1327 (1984).
- U. Middy, D. Luss, *J. Chem. Phys.* **102**, 5029 (1995).
- G. Vesper, F. Mertens, A. S. Mikhailov, R. Imbühl, *Phys. Rev. Lett.* **71**, 935 (1993).
- K. Rose, D. Battogtokh, A. S. Mikhailov, R. Imbühl, W. Engel, A. M. Bradshaw, *Phys. Rev. Lett.* **76**, 3582 (1996).
- A. von Oertzen, H. H. Rotermund, A. S. Mikhailov, G. Ertl, *J. Phys. Chem. B* **104**, 3155 (2000).
- V. K. Vanag, L. Yang, M. Dolnik, A. M. Zhabotinsky, I. R. Epstein, *Nature* **406**, 389 (2000).
- A. L. Lin et al., *Phys. Rev. Lett.* **84**, 4240 (2000).
- Y. Kuramoto, *Chemical Oscillations, Waves, and Turbulence* (Springer, Berlin, 1984).
- S. Jakubith, H. H. Rotermund, W. Engel, A. von Oertzen, G. Ertl, *Phys. Rev. Lett.* **65**, 3013 (1990).
- R. Imbühl, G. Ertl, *Chem. Rev.* **95**, 697 (1995).

20. Q. Ouyang, J.-M. Flesseles, *Nature* **379**, 143 (1996).
21. D. Battogtokh, A. S. Mikhailov, *Physica D* **90**, 84 (1996).
22. D. Battogtokh, A. Preusser, A. S. Mikhailov, *Physica D* **106**, 327 (1997).
23. H. H. Rotermund, W. Engel, M. Kordesch, G. Ertl, *Nature* **343**, 355 (1990).
24. H. H. Rotermund, *Surf. Sci. Rep.* **29**, 265 (1997).
25. The apparatus is equipped with low-energy electron diffraction, Auger electron spectroscopy, differentially pumped quadrupole mass spectroscopy, Ar-ion sputtering, and resistive sample heating. Using microlithography methods, we deposited a thin Ti layer surrounding areas of clean Pt. In situ oxidation of the Ti layer in the UHV

- chamber produces a TiO<sub>2</sub> layer. Because TiO<sub>2</sub> is not catalytically active for the CO oxidation, isolated surface reactors could thus be created. Such isolated prefabricated reactors of various sizes occupy ~80% of the entire sample surface. For the experiment, a 1-mm<sup>2</sup> reactive region is chosen. The sample is prepared by repeated cycles of Ne sputtering and O<sub>2</sub> treatment at 470 K and subsequent annealing to 750 K.
26. The instrument's field-of-view is chosen at 500 μm in diameter, and the spatial resolution of images is typically 1 μm. The PEEM images are recorded by a video camera at a rate of 40 ms per frame.
27. The PEEM intensity is defined so that the darker image areas have a higher intensity.

28. M. Kim *et al.*, unpublished data.
29. K. Krischer, M. Eiswirth, G. Ertl, *J. Chem. Phys.* **96**, 9161 (1992).
30. A. von Oertzen, A. S. Mikhailov, H. H. Rotermund, G. Ertl, *J. Phys. Chem. B* **102**, 4966 (1998).
31. Y. Pomeau, *Physica D* **23**, 3 (1986).
32. M. Argentina, P. Coulet, *Phys. Rev. E* **56**, R2359 (1997).
33. We gratefully acknowledge Y. Kevrekidis for help with microlithographic fabrication of the crystal samples used in these experiments.

1 February 2001; accepted 9 April 2001

## Bacterial Recognition of Mineral Surfaces: Nanoscale Interactions Between *Shewanella* and α-FeOOH

Steven K. Lower,<sup>1\*</sup> Michael F. Hochella Jr.,<sup>1</sup> Terry J. Beveridge<sup>2</sup>

Force microscopy has been used to quantitatively measure the infinitesimal forces that characterize interactions between *Shewanella oneidensis* (a dissimilatory metal-reducing bacterium) and goethite (α-FeOOH), both commonly found in Earth near-surface environments. Force measurements with subnanonewton resolution were made in real time with living cells under aerobic and anaerobic solutions as a function of the distance, in nanometers, between a cell and the mineral surface. Energy values [in attojoules (10<sup>-18</sup> joules)] derived from these measurements show that the affinity between *S. oneidensis* and goethite rapidly increases by two to five times under anaerobic conditions in which electron transfer from bacterium to mineral is expected. Specific signatures in the force curves suggest that a 150-kilodalton putative iron reductase is mobilized within the outer membrane of *S. oneidensis* and specifically interacts with the goethite surface to facilitate the electron transfer process.

The Fe(II)-Fe(III) redox cycle represents a major energy flux at Earth's surface. A critical component of this system is the reduction of iron-containing minerals by biological processes (1, 2). *Shewanella*—a Gram-negative, dissimilatory metal-reducing bacterium found in soils, sediments, surface waters, and ground waters—is able to conserve energy for growth by using oxygen or ferric iron as a terminal electron acceptor (3, 4). In many natural environments, oxygen is in limited supply, but Fe(III) is present as a major element in the crystal structure of minerals. Hence, dissimilatory metal-reducing bacteria often oxidize various carbon substrates by reductively dissolving Fe(III)-containing minerals, the most ubiquitous in the near-

surface environments being iron oxyhydroxides (such as ferrihydrite, goethite, and hematite) (5–12). This affects a wide array of processes, including the biogeochemical cycle of iron and phosphorus, the oxidation of natural and anthropogenic carbon sources, biocorrosion, and the release of heavy metals associated with iron oxyhydroxides.

The dissimilatory reduction of iron-containing minerals presents a rather unique situation because, unlike oxygen, Fe(III) in a solid form cannot diffuse across the cell wall to the plasma membrane which, in most bacteria, houses the proteins involved in electron transfer, proton translocation, and the subsequent generation of adenosine triphosphate. Microorganisms like *Shewanella* may be able to generate two energized membranes using a unique system of proteins that shuttle electrons from an energy source in the cytoplasm, across the plasma membrane and periplasmic space, to the outer membrane (13, 14). Once in the outer membrane, iron reductases appear to transfer electrons directly to Fe(III) in the crystal structure of minerals, causing a weakening of the iron-oxygen bond and reductive dissolution of the mineral (6, 15–18). A great deal of research has

focused independently on either the microbiological or mineralogical aspects of the interaction between *Shewanella* and iron oxyhydroxides. However, few studies have been conducted on the interface between the bacterium and iron-containing minerals. It is this interface, delineated by chemical and structural features on the surface of the organism (such as concentration and localization of cytochromes and reductases and the physical structure of the outer membrane) and the mineral surface (such as density and coordination of iron-oxide moieties, surface microtopography, and crystallographic orientation), which probably has a major impact on the kinetics and extent of bacterial reduction of Fe(III) minerals.

We used biological force microscopy (19, 20) to probe the interface between a living cell of *Shewanella oneidensis*, formerly classified as *S. putrefaciens* MR-1 (21), and the (010) surfaces of goethite (α-FeOOH) and diaspore (α-AlOOH, which is isostructural with goethite and has surface properties such as charge and hydrophobicity that are similar to those of goethite) at the nanoscale level in anaerobic and aerobic solutions. *S. oneidensis* was grown under anaerobic conditions using lactate as the carbon and energy source and Fe(III)-citrate as the electron acceptor (22). To preserve the natural, complex biomolecular network on the surface of the bacteria, fully functional cells (measuring 0.5 by 2 μm) were linked in their native state to a small bead (radius 5 μm) situated on the end of a silicon nitride cantilever thereby creating a biologically active force probe (23). A commercial force microscope (NanoScope IIIa Multimode scanning probe microscope, Digital Instruments, Santa Barbara, CA) was used to measure the deflection of a biologically active force probe by reflecting a laser off the top of the cantilever and into a photodiode detector while an oriented mineral crystal, mounted on a piezoelectric scanner, was translated toward (generating approach data), made contact with, and was subsequently retracted from (generating retraction data) a bacterium on the probe (24). Photodiode response (in volts) was converted to cantilever deflection (in meters) using a conversion factor (in meters per volt) determined from the photodiode shift voltage (25). Cantilever deflection was multiplied by the cantilever spring constant [ $k_{sp} = 0.07 \text{ N m}^{-1}$ , determined

<sup>1</sup>NanoGeoscience and Technology Laboratory, Department of Geological Sciences, Virginia Polytechnic Institute and State University, Blacksburg, VA 24061, USA. <sup>2</sup>Department of Microbiology, College of Biological Science, University of Guelph, Guelph, Ontario N1G 2W1, Canada.

\*To whom correspondence should be addressed. E-mail: slower@vt.edu Present address: Department of Geology, University of Maryland, College Park, MD 20742, USA.